ELSEVIER

Materials Science and Engineering B 117 (2005) 27–36

MATERIALS SCIENCE & ENGINEERING B

www.elsevier.com/locate/mseb

Microwave-absorbing characteristics for the composites of thermal-plastic polyurethane (TPU)-bonded NiZn-ferrites prepared by combustion synthesis method

Cheng-Hsiung Peng[a], Chyi-Ching Hwang[b,*], Jun Wan[b], Jih-Sheng Tsai[b], San-Yuan Chen[a]

[a] *Department of Materials Science and Engineering, National Chao Tung University, Hsinchu 300, Taiwan*
[b] *Department of Applied Chemistry, Chung Cheng Institute of Technology, Tashi Jen, Taoyuan 335, Taiwan*

Received 6 June 2004; received in revised form 6 October 2004; accepted 14 October 2004

Abstract

NiZn ferrite with the chemical formula $Ni_{0.5-x}Zn_{0.5-x}M_{2x}Fe_2O_4$ (M = Co, Cu, or Mg, and $x = 0$ or 0.05) was synthesized by a combustion synthesis method using metal nitrates and urea ($(NH_2)_2CO$) as reactants. The nanocrystallite of these materials were mixed with a thermal-plastic polyurethane (TPU) elastomer to be converted into a microwave-absorbing composite. The complex relative permittivity ($\varepsilon_r = \varepsilon' - j\varepsilon''$) and permeability ($\mu_r = \mu' - j\mu''$) of the absorber were measured in a frequency range of 2–12 GHz. The reflection loss (R.L.), matching frequency (f_m) and matching thickness (d_m) were calculated using the theory of the absorbing wall. Effects of both the particle size of ferrite and the dopant presented in the ferrite on the electromagnetic properties and microwave-absorbing characteristics were investigated. It was found that nanoparticles around 40 nm exhibit higher reflection loss than both those obtained from micro-sized powders and those with size less than 25 nm. Also, it was shown that the Co-doped, Mg-doped, and Cu-doped NiZn ferrite-TPU composites could be designed to be more negative than −20 dB, in a frequency range of 2–12 GHz, to become promising materials for microwave-absorbing application. These doped ferrite-containing composites have more effective microwave-absorbing characteristics compared to undoped one.

Keywords: NiZn ferrites; Microwave absorbers; Reflection loss; Combustion synthesis

1. Introduction

Much attention has been attracted by microwave-absorbing materials due to the facts that they can absorb energy from microwave and that they can be widely used in the stealth technology of aircraft, television image interference of high-rise buildings, and microwave dark-room and protection etc. [1,2]. Extensive study has been carried out to develop microwave-absorbing materials with high efficiency and new absorption materials [3–5]. One criterion in selecting the absorbing material is to discover the location of its natural resonance region. Thus, a study of the frequency dependencies of the complex relative permittivity ($\varepsilon_r = \varepsilon' - j\varepsilon''$) and permeability ($\mu_r = \mu' - j\mu''$) on the absorbing material has been a field of interest.

In the past, the spinel ferrites have been utilized as absorbing materials in various forms for many years. Also, the ferrite-polymer composites are useful as absorbers due to their lightweight, low cost, and good design flexibility [1,5,6]. Among the spinel ferrites, NiZn ferrites are commercially used as electromagnetic devices operated in high frequencies (>10 MHz), arising from the fact that metal dopants can be used to modify the electromagnetic properties of NiZn ferrites by increasing the resistivity and permeability [7]. For this purpose, some attempts were made to verify the correlation between the material constants, ε_r and μ_r, and microwave absorption in the sintered ferrites that contain divalent metal ions [6–9].

Recently, the research pursuing to nanocrystalline materials and their properties has been given much attention

* Corresponding author. Tel.: +886 3 3891716x312; fax: +886 3 3892494.
E-mail address: cchwang1@ccit.edu.tw (C.-C. Hwang).

0921-5107/$ – see front matter © 2004 Elsevier B.V. All rights reserved.
doi:10.1016/j.mseb.2004.10.022

and it is well known that nano-scale particles possess distinctive physical and chemical properties because of their nano-sized crystallite, large surface area and different surface properties (such as surface defect) etc. Yet, a variety of wet-chemical methods (such as sol–gel, co-precipatation and hydrothermal, etc.) have been reported to be effective in generating nano-sized and homogeneous powders of ceramic oxides [10–12]. However, relatively complex schedules, expensive precursors, and low production rate are the common problems of the wet-chemical method [13]. In the past decade, a solution combustion method has been narrated and utilized to synthesize simple and/or mixed metal oxides [14–17]. With this method, the heating and evaporation of desired metal nitrate solution employing an organic compound can result in self-firing to generate heat by exothermic reaction. This liberated heat is used to synthesize the ceramic oxide powders. Together, this method has advantages of applying inexpensive raw materials and maintaining a relatively straightforward preparation process, and achieving a fine powder with high homogeneity. In addition, the process of combustion reaction is relatively quick as compared to other synthesis techniques. This process with its fast pace in ascending and descending the temperature can produce meta-stable phase, un-equilibrium phase and products of tiny grains; therefore, superior properties are attainable [18].

In our previous research, a further modified combustion synthesis method has been developed for preparation of nanocrystalline ceramic oxides [19]. Utilization of an organic compound (e.g., glycine, urea, citric acid, alanine or carbohydrazide) and metal nitrates in conjunction with mixing the reactants directly without adding water are the key techniques of this method. It was found that the sinterability and soft-magnetic properties of the resultant NiZn ferrite powder are superior to those obtained by other methods.

Since there was not much literature reporting the application of using combustion method to synthesize NiZn ferrites in regard to making electromagnetic wave absorbers, we continue our research to use combustion synthesis method to synthesize NiZn ferrite and Mg-, Co-, and Cu-doped NiZn ferrites (chemical formula: $Ni_{0.5-x}Zn_{0.5-x}M_{2x}Fe_2O_4$, M = Mg, Co or Cu, and $x = 0$ or 0.05), and then the resultant ferrite powders were blended with a thermal-plastic polyurethane (TPU) elastomer to be made into microwave-absorbing composites and used in our relevant research. In this work, the effects of both the particle size of ferrite and the dopant presented in the ferrite on the electromagnetic properties and microwave-absorbing characteristics are evaluated.

2. Experimental procedure

The flow chart of the experimental procedure is shown in Fig. 1.

2.1. Preparation of ferrite

Ferrite powders were prepared by an amount of 25 g per batch from an exothermic reaction using mixtures of metal nitrates (purity: >99%, Aldrich) and urea ($(NH_2)_2CO$, purity: 99.5%, Alfa). Reactants were directly mixed at an 'equivalent stoichiometric ratio' without adding water. Note that the 'equivalent stoichiometric ratio' is designated as the oxygen content of metallic nitrates that can be completely reacted to oxidize/consume urea exactly. The reactant mixture can easily absorb moisture from the air and become a slurry substance, since metallic nitrates possess hygroscopicity. This slurry mixture was homogenized and heated on a hot plate at ~230 °C to dehydrate until self-ignition was taken place. Then, the dried mixture was ignited at room temperature to start combustion reaction, giving rise to the evolution of a large volume of gases and producing a dry, loose, and voluminous ash. When complete combustion is assumed, the reaction equation can be expressed (greatly-simplified) as follows:

$$(0.5-x)\mathrm{Ni(NO_3)_2} + (0.5-x)\mathrm{Zn(NO_3)_2} + 2x\mathrm{M(NO_3)_2} + 2\mathrm{Fe(NO_3)_3} + 6.67\mathrm{CO(NH_2)_2} \xrightarrow{\Delta} \mathrm{Ni_{0.5-x}Zn_{0.5-x}M_{2x}Fe_2O_4} + 6.67\mathrm{CO_2} + 10.67\mathrm{N_2} + 13.34\mathrm{H_2O} \quad (1)$$

To understand the influences of heat treatment on grain size and magnetic properties, a portion of the as-synthesized ferrite powders was annealed at 500 °C and 900 °C for 1 h. For comparison, a commercial $Ni_{0.5}Zn_{0.5}Fe_2O_4$ (purity: 99%, average diameter: 1.5 μm, source: Core connector Co., Taiwan) manufactured by the conventional mixed oxide method was also used in the present study.

2.2. Characterization of ferrite

Phase formation of product was identified by using X-ray diffraction (XRD; SIEMENS D5000) with Cu Kα radiation (λ = 0.15418 nm). The crystallite size (D) of NiZn ferrite was calculated from the diffraction peak of the (3 1 1) plane from the XRD profile, in accordance with the Debye–Scherrer formula [20]:

$$D = \frac{0.9\lambda}{(\beta \cos\theta)} \quad (2)$$

where λ is the X-ray wavelength, β is the half-maximum breadth, and θ is the Bragg angle of the (3 1 1) plane. The morphological features and the electron diffraction patterns of the ferrite powders were imaged by transmission electronic microscope (TEM; Hitachi H-7100, Japan). Vibrating sample magnetometer (VSM; Toei, VSM-5) was used to determine the hysteresis loops of ferrite powders at room temperature.

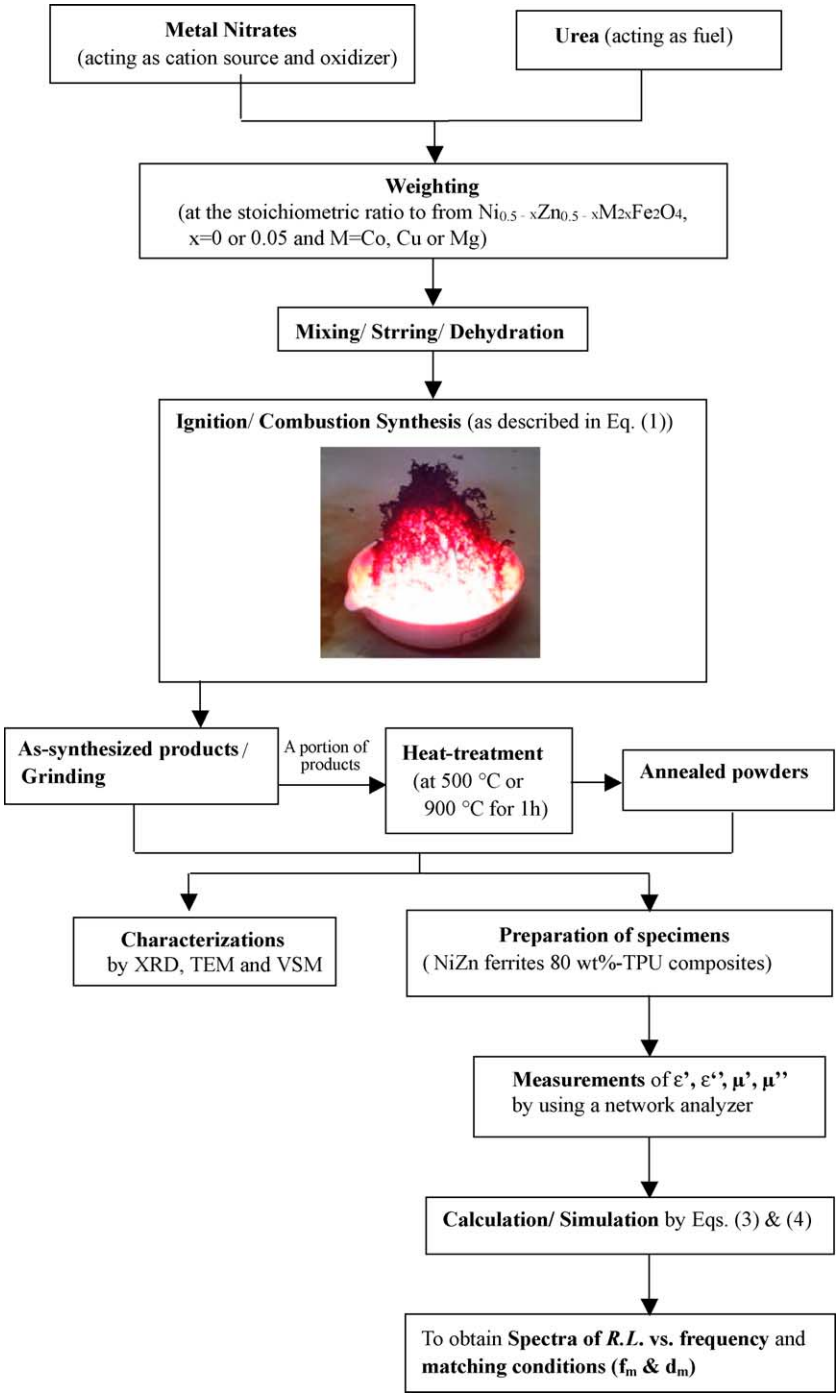

Fig. 1. Flow chart of experimental procedure in this study.

2.3. *Measurement of microwave-absorbing behavior for ferrite-TPU composite*

The absorbing composite materials were prepared by molding and curing the mixture of ferrite powders and a TPU elastomer. TPU was used as a polymer matrix due to its good flexibility and high filler content. It becomes obvious that high filler content would enhance the complex permittivity of ferrite-polymer composite [21]. The mixing ratio of ferrite-to-TPU was fixed at 80% by weight. The testing specimens have a toroidal shape with both thickness being 1 mm and outer and inner diameters being 7.0 and 3.0 mm, respectively. The measurements of ε', ε'', μ' and μ'' versus frequency were made by coaxial reflection/ transmission method using a Hewlett-Packard Network Analyzer (Model: HP/8510C) in a 2–12 GHz frequency range.

The absorbing characteristics can be represented as the reflection loss (R.L.), to be described as [22]:

$$\text{R.L.(dB)} = 20\log_{10}\left|\frac{(Z_{\text{in}}-1)}{(Z_{\text{in}}+1)}\right| \quad (3)$$

$$Z_{\text{in}} = \left(\frac{\mu_{\text{r}}}{\varepsilon_{\text{r}}}\right)^{1/2}\tanh\left[j\left(\frac{2\pi fd}{C}\right)\left(\frac{\mu_{\text{r}}}{\varepsilon_{\text{r}}}\right)^{1/2}\right] \quad (4)$$

where Z_{in} is the normalized input impedance relating to the impedance in free space, $\varepsilon_{\text{r}} = \varepsilon' - j\varepsilon''$, $\mu_{\text{r}} = \mu' - j\mu''$ is the complex relative permeability and permittivity of the material, d is the thickness of the absorber, and C and f are the velocity of light and the frequency of microwave in free space, respectively.

The impedance matching condition is given by $Z_{\text{in}} = 1$ to represent the perfect absorbing properties. The impedance matching condition is determined by the combinations of six parameters ε', ε'', μ', μ'', f and d. Also, knowing the ε_{r} and μ_{r}, the R.L. value versus frequency can be evaluated at a specified thickness.

3. Results

3.1. Phase Identification

Fig. 2 shows the crystalline phases of as-synthesized undoped and doped ferrite powders. It is observed that only single spinel phase exists. In the doped ferrite cases, the dopants of Co^{2+}, Cu^{2+} or Mg^{2+} seem to dissolve/arrange in the spinel structure to fulfill the formation of single spinel phase. It is generally recognized that the vacancy sites of partial deprivation of Ni^{2+} and Zn^{2+} can be filled by these dopant ions arising from the facts that the ionic radii of Co^{2+}, Cu^{2+} and Mg^{2+} are actually 0.060 nm, 0.058 nm and 0.057 nm, respectively, which are close to the ionic radii of Ni^{2+} (0.055 nm) and Zn^{2+} (0.060 nm). (These ionic radii mentioned above are simply for the case of coordination number (C.N.) = 4. When C.N. = 6, the ionic radii of Ni^{2+}, Zn^{2+}, Co^{2+}, Cu^{2+} and Mg^{2+} are 0.069 nm, 0.074 nm, 0.075 nm, 0.077 nm and 0.072 nm, respectively [23], which are nearly equal to each other.) Fig. 3 shows the more narrow peaks of NiZn ferrites after annealing at 500 °C and 900 °C for 1 h. It is expected that crystallite size after annealing will become larger due to grain growth. Table 1 depicts the result of the crystallite size determined by XRD. One can observe from this table that the grain size increases with respect to the increase of annealing temperature.

3.2. Morphology observation

The morphology of as-synthesized NiZn ferrite powders and the powder products annealed at 500 °C for 1 h with their corresponding electron diffraction patterns are shown in Fig. 4. The crystallite sizes were estimated to be ~20 nm for the as-synthesized powders and ~35–45 nm for the annealed

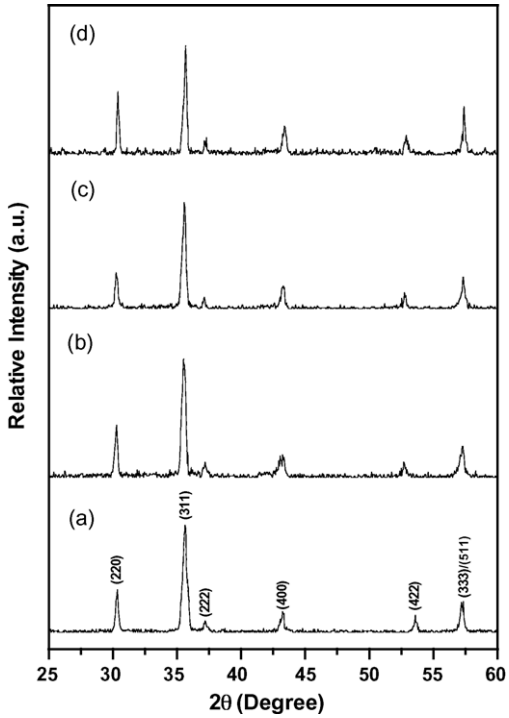

Fig. 2. XRD patterns of as-synthesized NiZn ferrite powders. (a) Undoped, (b) Co-doped, (c) Cu-doped, and (d) Mg-doped.

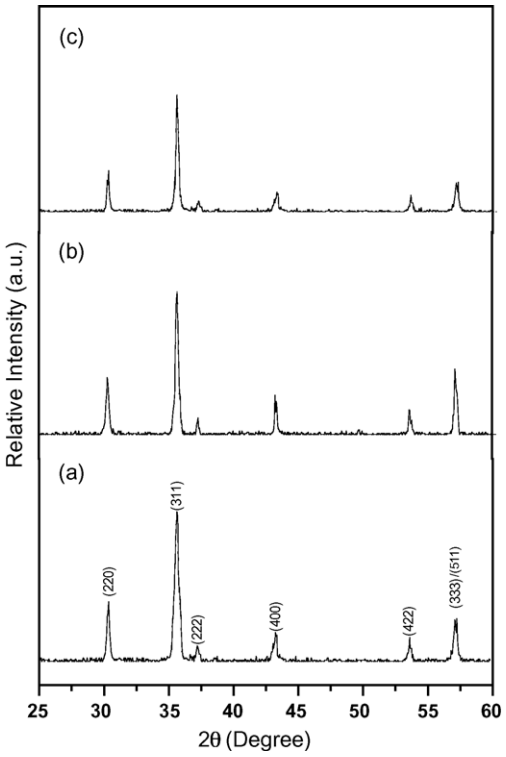

Fig. 3. XRD patterns of as-synthesized $Ni_{0.5}Zn_{0.5}Fe_2O_4$ powders. (a) Without heat treatment, (b) annealed at 500 °C for 1 h, and (c) annealed at 900 °C for 1 h.

Table 1
Grain sizes of ferrite and detail data for hysteresis loops shown in Fig. 3

Specimen	D^a (nm)	H_c (Oe)	M_s (emu/g)	M_r (emu/g)	A_H (kJ/m^3)
Synthesized ferrite					
Without heat-treatment	25	52.12	44.24	3.421	41.25
Annealed at 500 °C/1 h	45	65.82	31.35	3.216	57.75
Annealed at 900 °C/1 h	80	28.01	38.82	1.489	34.17
Commercial ferrite	–	24.12	36.08	0.950	37.73

[a] Evaluated by the Debye–Scherrer formula.

ones in regard to which they are about the same sizes as the ones estimated by using XRD method. In addition, diffraction patterns indicate that the heat-treated powders have a higher degree of crystallinity than do the as-synthesized powders since their diffraction rings are sharper and brighter as compared with those of the powders without heat treatment.

3.3. Measurement of hysteresis loop

The hysteresis loop shown in Fig. 5 illustrates what are the real traces of the magnetic behavior of the as-synthesized NiZn ferrite as well as the ferrite samples that were annealed at 500 °C and 900 °C for 1 h. Table 1 presents the relevant data. It is interesting to recognize that the powders after annealing at 500 °C possess the largest coercive force (H_c), the largest hysteresis loop area (A_H) and the smallest remanence (M_r) than those of other samples, while the former two factors may lead to the largest hysteresis loss [24]. Moreover, the saturated magnetization (M_s) values of the calcined NiZn ferrites are smaller than that of the one without heat treatment.

Fig. 6 shows the hysteresis loops of the undoped, Co-doped, Cu-doped, and Mg-doped NiZn ferrites annealed at

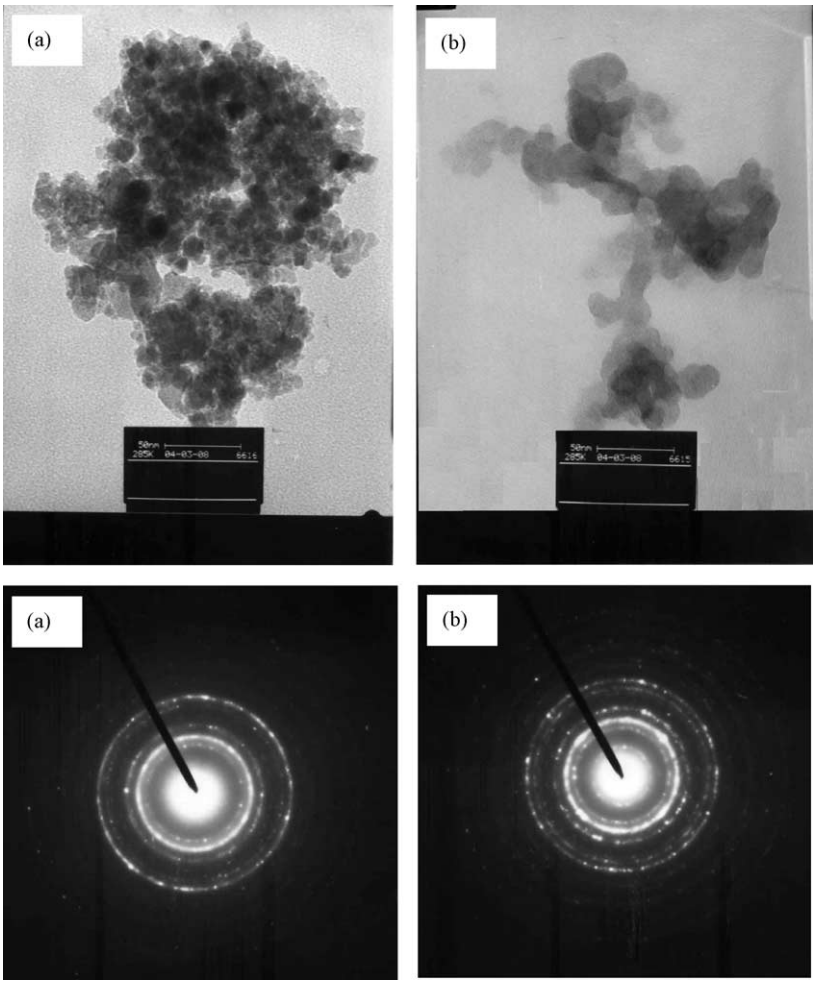

Fig. 4. TEM images of synthesized powders with corresponding diffraction patterns. (a) Without heat treatment, and (b) annealed at 500 °C for 1 h (Taken at the same operation conditions).

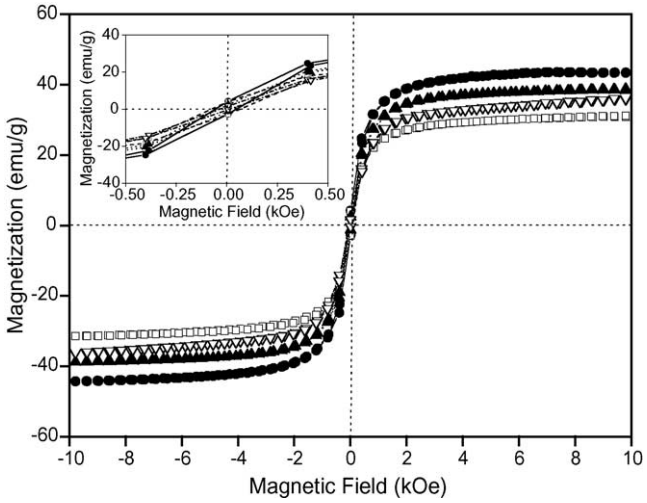

Fig. 5. Room-temperature hysteresis loops of $Ni_{0.5}Zn_{0.5}Fe_2O_4$ powders. (●) As-synthesized ferrite without heat treatment, (□) synthesized ferrite annealed at 500 °C for 1 h, (▲) synthesized ferrite annealed at 900 °C for 1 h, and (▽) commercial ferrite. (A plot magnifying the vicinity of the origin is inset into Fig. 4. The values of H_c (i.e., the intersection point on positive x-axis) and M_r (i.e., the intercept on positive y-axis) for each specimen can be observed).

500 °C for 1 h. The data presented in Fig. 6 and Table 2 illustrate that the hysteresis parameters of these doped NiZn ferrites are considerably larger than those of the undoped one. Evidently, introducing these dopants can modify the magnetic properties of NiZn ferrite. It is thus expected that the composites fabricated by using doped-NiZn ferrite might possess different microwave-absorbing characteristics when compared with the composite of undoped NiZn ferrite-TPU.

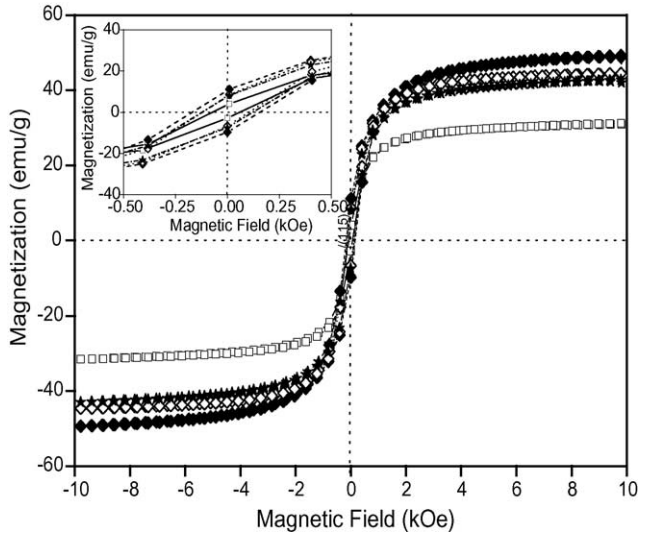

Fig. 6. Room-temperature hysteresis loops of synthesized doped- and undoped-ferrite powders annealed at 500 °C for 1 h. (□) Undoped, (♦) Co-doped, (◊) Cu-doped, and (⋆) Mg-doped. (A zoom plot showing the vicinity of the origin is inset into Fig. 5.The values of H_c (i.e., the intersection point on positive x-axis) and M_r (i.e., the intercept on positive y-axis) for each specimen can be observed.).

3.4. Measurement of electromagnetic property

Fig. 7(a–d) manifests the real part and the imaginary part of the relative permittivity (ε' and ε'') and permeability (μ' and μ'') spectra for $Ni_{0.5}Zn_{0.5}Fe_2O_4$-TPU composites. The real part and the imaginary part of permittivity are almost constant ($\varepsilon' = 6$–7 and $\varepsilon'' = 0.45$–0.65, respectively). This is most likely to be caused by the intrinsically small dielectric loss tangent ($\tan\delta_\varepsilon$) of the ferrite powder used in this study. The values of μ' and μ'' depend on the frequency and calcination temperature. The spectrum of μ' exhibits a fall at the beginning and then remains constant in 5–12 GHz, whereas the μ'' decreases with increasing frequency.

Fig. 8 gives the relative permittivity and the relative permeability spectra for doped and undoped ferrite-TPU composites. The real part and imaginary part of permittivity remain practically constant and they depend on the dopant to be varied from 6 to 7.5 and from 0.45 to 1.0, respectively. With increasing frequency, the μ' exhibits a decreasing tendency (except for Co-doped sample) in the order of undoped > Mg-doped > Cu-doped. The maximum value of μ'' can be shifted to higher frequency in the order of Co-doped > Cu-doped > Mg-doped > undoped. In addition, the value of μ'' is also augmented in such an order, especially in the high-frequency region (>8 GHz).

3.5. Reflection loss

Fig. 9 shows the reflection losses and the matching frequencies of the NiZn ferrite (annealed at 500 °C for 1 h)-TPU composite, which can be obtained by using Eqs. (3) and (4). The matching frequency (f_m) is equal to 3.16 GHz in the lower-frequency region and it is equal to 9.43 GHz in the higher-frequency region. The corresponding values of matching thickness (d_m) are 5.92 mm and 2.13 mm, respectively. Table 3 lists the data of absorption characteristics for the absorbing composites fabricated from the commercial NiZn ferrite, as-synthesized and annealed at 500 °C and 900 °C for 1 h. It is clear that these NiZn ferrite-TPU composites can be considered as a microwave-absorbing material in ∼2–4 GHz lower-frequency range and in ∼9–10 GHz higher-frequency range. In particular, the NiZn ferrite after annealing at 500 °C for 1 h exhibits the largest reflection loss and the widest bandwidth than those obtained from other specimens. This phenomenon, coupled with the results presented in Table 1, suggests that the crystallite size of NiZn ferrite has significant effects on magnetic properties and microwave-absorbing characteristics.

Table 4 shows the absorption efficiency for the undoped, Co-doped, Mg-doped, and Cu-doped NiZn ferrite -TPU composites to be obtained by taking the specified thickness of 2 mm and 5 mm, respectively. It shows that the reflection loss of these composites could be designed to be more negative than −20 dB in the frequency range of 2–12 GHz. In addition, it is evident that the doped ferrite-containing composites have much more effective electromagnetic absorp-

Table 2
Detail data for hysteresis loops shown in Fig. 4

Specimen[a]	H_c (Oe)	M_s (emu/g)	M_r (emu/g)	A_H (kJ/m^3)
Doped ferrite				
$Ni_{0.45}Zn_{0.45}Co_{0.1}Fe_2O_4$	161.4	49.30	10.04	191.2
$Ni_{0.45}Zn_{0.45}Cu_{0.1}Fe_2O_4$	112.3	44.53	7.431	126.8
$Ni_{0.45}Zn_{0.45}Mg_{0.1}Fe_2O_4$	112.2	42.85	6.907	116.4
Undoped ferrite ($Ni_{0.5}Zn_{0.5}Fe_2O_4$)	65.82	31.35	3.216	57.75

[a] As-synthesized ferrites calcined at 500 °C for 1 h.

tion effects. The effect of Cu, Mg, and Co to be added in NiZn ferrite can be understood from their changes in premittivity and permeability in addition to their hysteresis characteristics and it will be discussed briefly in the following section.

4. Discussion

By using the combustion synthesis method and annealing process, we were able to fabricate NiZn-ferrite powders with particle size ranging from ~20 nm to a size approximately 80 nm. The commercial $Ni_{0.5}Zn_{0.5}Fe_2O_4$ powder with micro-scale size was also fabricated. From Fig. 4 and Table 3, it is found that the crystallite size obtained at calcinations temperature of 500 °C, which is ~35–45 nm, has better reflection loss and bandwidth than those acquired from greater particle size (in micro-sized range) or as-synthesized one (<25 nm). Recent report [25] claims that a critical particle size becomes available as transited from mono-magnetic-domain to multi-magnetic-domain to be close to 40 nm. In this transition stage, both domain wall motion and spin rotation are in operation us-

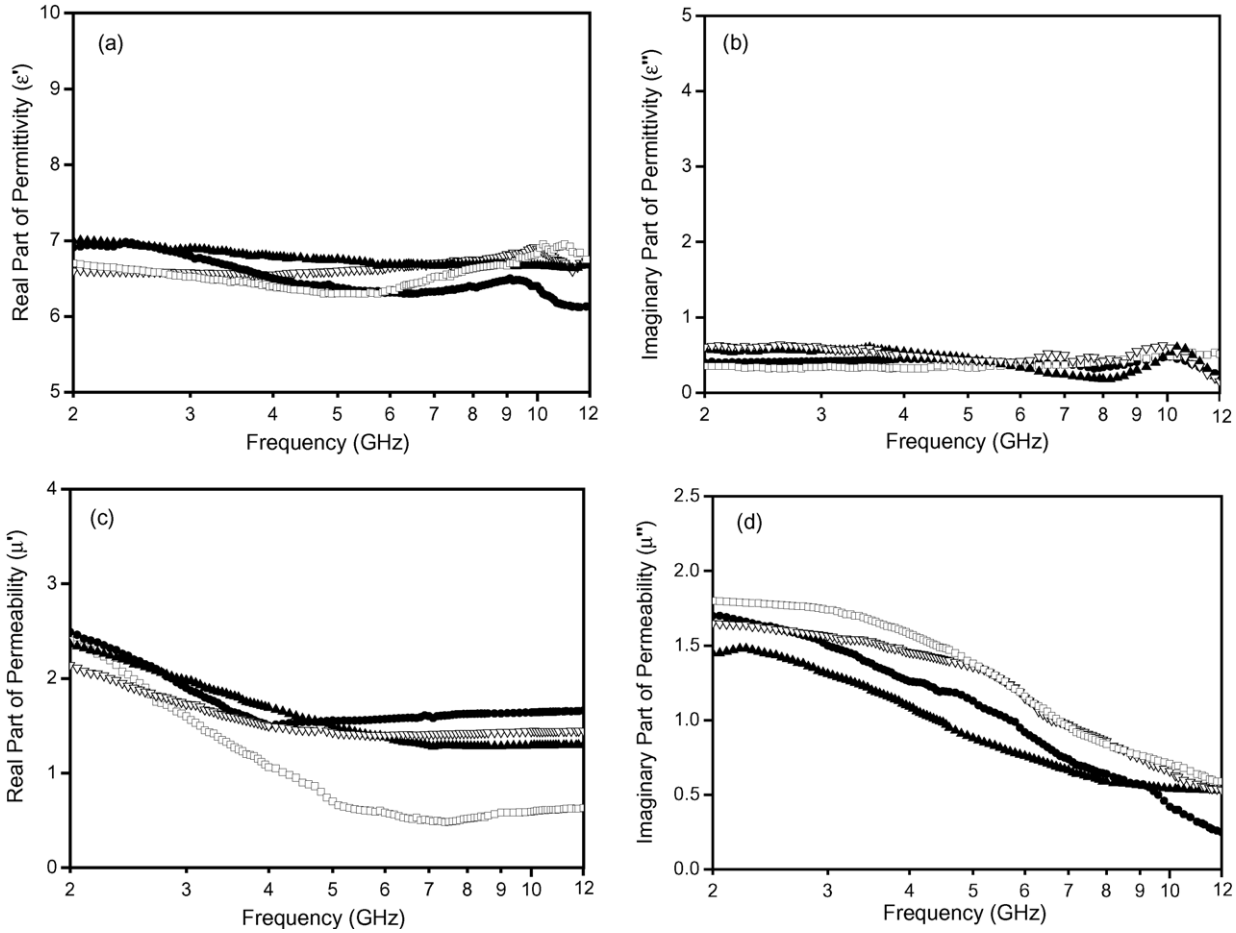

Fig. 7. Permittivity and permeability spectra of $Ni_{0.5}Zn_{0.5}Fe_2O_4$-TPU composites. (a) ε', (b) ε'', (c) μ', and (d) μ''. (●) As-synthesized ferrite without heat treatment, (□) synthesized ferrite annealed at 500 °C for 1 h, (▲) synthesized ferrite annealed at 900 °C for 1 h, and (▽) commercial ferrite.

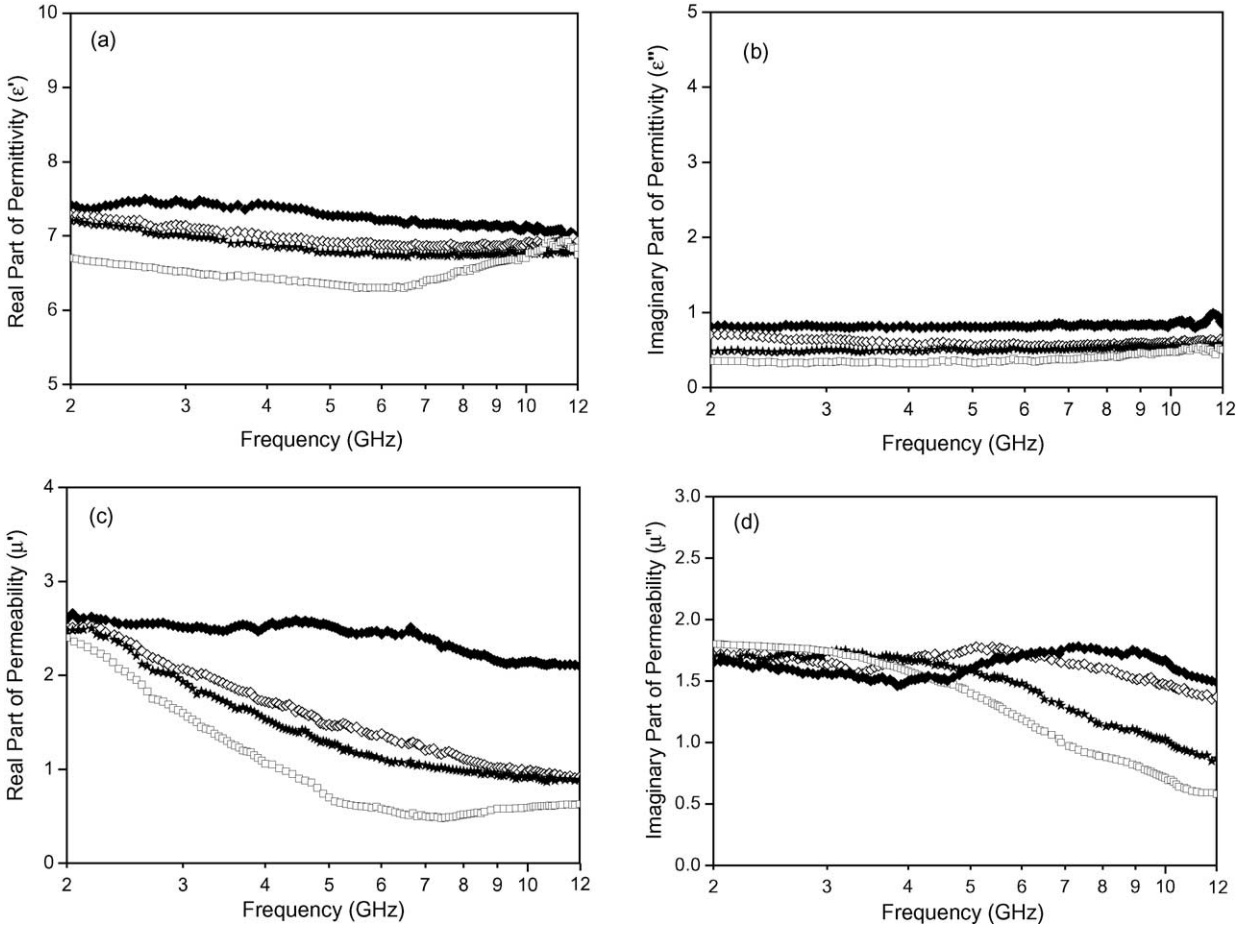

Fig. 8. Permittivity and permeability spectra of doped- and undoped-NiZn ferrite-TPU composites. (a) ε', (b) ε'', (c) μ', and (d) μ''. (□) Undoped, (♦) Co-doped, (◊) Cu-doped, and (⋆) Mg-doped. (All of these synthesized ferrites were annealed at 500 °C for 1 h.).

ing the magnetizing processes [26]. It is thought that for small crystallite size (as-synthesized ferrite without heat treatment) only spin resonance is observed, however, both spin rotation and domain wall can be operated with respect to large crystallite size (annealed at 500 °C and above). Not only can nano-sized powders increase unsaturated coordination, interface polarization, and multiple scatter near the size of transition stage (∼40 nm), but they also exist quantum size effect such as electronic energy level split. The Ref. [25] also indicates that in the transition stage from single domain to multidomain, coercive force reaches to a maximum, which may lead

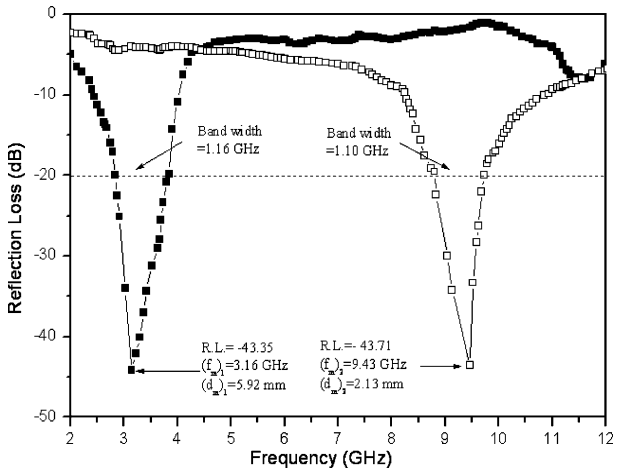

Fig. 9. Absorption characteristics of the $Ni_{0.5}Zn_{0.5}Fe_2O_4$-TPU composite with maximum attenuation. (All of the synthesized ferrite was annealed at 500 °C for 1 h.).

Table 3
Relationship between matching frequency and matching thickness in $Ni_{0.5}Zn_{0.5}Fe_2O_4$-TPU composites

Specimen	f_m (GH_Z)	d_m (mm)	R.L. (dB)	Bandwidth[a] (GH_Z)
Synthesized ferrite				
Without heat treatment	9.15	3.07	−32.38	0.74
	2.52	5.43	−35.62	0.85
Annealed at 500 °C/1 h	9.43	2.13	−43.71	1.10
	3.16	5.92	−43.35	1.16
Annealed at 900 °C/1 h	8.89	3.42	−29.47	0.69
	2.27	5.65	−31.03	0.73
Commercial ferrite	9.02	3.23	−31.81	0.70
	2.97	5.62	−33.46	0.79

[a] For R.L.≤20 dB.

Table 4
Reflection loss of composites made from synthesized doped and undoped ferrite powders annealed at 500 °C for 1 h

Specimen	R.L. (dB)		Location of maximum R.L. (GHz)		Band width[a] (GH_Z)	
	$d = 2$ mm	$d = 5$ mm	$d = 2$ mm	$d = 5$ mm	$d = 2$ mm	$d = 5$ mm
Co-doped NiZn ferrite	−30.74	−42.51	11.18	5.14	0.34	0.57
Cu-doped NiZn ferrite	−27.61	−37.07	10.52	5.58	0.21	0.43
Mg-doped NiZn ferrite	−23.41	−29.32	10.17	6.04	0.12	0.46
Undoped NiZn ferrite	−21.52	−24.34	9.52	5.82	0.10	0.33

[a] For R.L. ≤ 20 dB.

to large hysteresis attenuation and absorbing behavior. Our experimental results agree with this perspective.

On the other hand, when the M^{2+} ion (M = Co, Cu, or Mg) substitutions are introduced into the sublattices in the reversed NiZn spinel ferrite, it may occupy the octahedral sites in replacing the Zn^{2+} or Ni^{2+} ions due to their nearly the same radii. The strength of the superexchange interaction can be reduced whereas the magnetic moments can be improved, resulting in an increase in the spontaneous magnetization [27]. Some researches have been made also to verify that not only can the saturation magnetization (M_s) and coercive force (H_c) of NiZn ferrites be enhanced by substituting a portion of Zn^{2+} or Ni^{2+} ions by divalent metal ions such as cobalt, but also the initial permeability [6–9,28]. In this work, for the Co-doped, Cu-doped, and Mg-doped NiZn ferrite, the permeability and the hysteresis loop can be modified due to the presence of these dopants, which are in agreement with the statement mentioned above (see Table 2 and Fig. 6). The further-improved magnetic properties of these doped ferrites were also reported in Refs. [6–9,26], and thereby it would be instructive to suggest that the doped-ferrite compositions possess better absorbing characteristics when compared with the undoped one. This opinion may be verified using the data listed in Table 4.

In summary, in this work, the experimental results indicate that the grain size of the NiZn ferrites and the presence of the dopant affect the microwave-absorbing behavior of the ferrite-TPU composite. Therefore, the improved reflection losses were thought to be related to enhanced permeability, larger coercive force, and large hysteresis loop. These results can be attributed to be from the domain wall motion and spontaneous magnetization. Further investigation for the effects of both ferrite and dopant content on the relationship between the electromagnetic characteristics of nano-sized ferrite composites and their microwave-absorbing properties are underway and we will soon disclose where we stand.

5. Conclusion

In this study, we have carried out experiments to demonstrate the dependence of particle size of NiZn ferrite on the reflection loss of ferrite-TPU composite by using combustion synthesized powders (20–80 nm) and commercial micro-sized powders. It is found that nanocrystallite of NiZn ferrite around 35–45 nm exhibit higher reflection loss than both those of micro-sized powders and those with size less than 25 nm. In addition, the Co-doped, Mg-doped, and Cu-doped NiZn ferrite-TPU composites have more effective absorption effect than the undoped one. These composites could be designed to be more negative than −20 dB in a frequency range of 2–12 GHz to be able to become promising materials for microwave-absorbing application.

Acknowledgements

Support for this research by the National Science Council of the Republic of China under Grant no. NSC 93-2623-7-014-005 is gratefully acknowledged.

References

[1] M. Pardavi-Horvath, J. Magn. Magn. Mater. 215-216 (2000) 171–183.
[2] J.Y. Shin, J.H. Oh, IEEE Trans. Magn. 29 (1993) 3437–3439.
[3] S. Ruan, B. Xu, H. Suo, F. Wu, S. Xiang, M. Zhao, J. Magn. Magn. Mater. 212 (2000) 175–177.
[4] V.K. Babbar, A. Razdan, R.A. Puri, T.C. Goel, J. Appl. Phys. 87 (2000) 4362–4366.
[5] A. Verma, A.K. Saxena, D.C. Dube, J. Magn. Magn. Mater. 263 (2003) 228–234.
[6] S.B. Cho, D.H. Kang, J.H. Oh, J. Mater. Sci. 31 (1996) 4719–4722.
[7] G.-J. Yin, S.-B. Liao, IEEE Trans. Magn. 27 (1991) 5459–5461.
[8] O.F. Caltun, L. Spinu, A. Sstancu, IEEE. Trans. Magn. 37 (2001) 2353–2355.
[9] M. Hisatoshi, Japanese patent No. 8012904 (1996).
[10] W.H. Lin, S.-K.J. Jean, C.S. Hwang, J. Mater. Res. 14 (1999) 204–208.
[11] J. Schäfer, W. Sigmund, S. Roy, F. Aldinder, J. Mater. Res. 12 (1997) 2518–2521.
[12] P.S.A. Kumar, J.J. Shrotri, C.E. Deshpande, J. Appl. Phys. 81 (1997) 4788–4790.
[13] Z. Yue, J. Zhou, L. Li, H. Zhang, Z. Gui, J. Magn. Magn. Mater. 208 (2000) 55–60.
[14] T. Mimani, K.C. Patil, Mater. Phys. Mech. 4 (2001) 134–136.
[15] R.D. Purohit, S. Saha, A.K. Tyagi, J. Nucl. Mater. 288 (2001) 7–10.
[16] Y.P. Fu, C.H. Lin, J. Magn. Magn. Mater. 251 (2002) 74–79.
[17] A.C.F.M. Costa, E. Tortella, M.R. Morelli, R.H.G.A. Kiminami, J. Magn. Magn. Mater. 256 (2003) 174–182.
[18] A.G. Merzhanov, Int. J. Self-Propag. High-Temp Synth. 6 (1997) 119–142.
[19] C.C. Hwang, T.Y. Wu, J. Wan, J.S. Tsai, Mater. Sci. Eng. B 111 (2004) 49–56.

[20] H.P. Klug, L.E. Alexander, X-ray Diffraction Procedures for Polycrystalline and Amorphous Materials, Wiley, New York, NY, 1997, p. 637.
[21] B.T. Lee, H.C. Kim, Jpn. J. Appl. Phys. 35 (1996) 3401–3406.
[22] Y. Michielssen, J.-M. Sager, S. Ranjithan, R. Mittra, IEEE Trans. Microwave Theory Tech. 41 (1993) 1024–1031.
[23] Y.M. Chiang, D.P. Brinie III, W.D. Kingery, Physical Ceramics: Principles for Ceramic Science and Engineering, John Wiley & Sons, New York, NY, 1997, p. 16.
[24] T.S. Chin (Ed.), Handbook of Magnetic Technologies, Chinese Association for Magnetic Technology, 2002, pp. 118–144.
[25] A.S. Albuquerque, J.D. Ardisson, W.A.A. Macedo, J. Appl. Phys. 87 (2000) 4352–4357.
[26] T. Tsutaoka, L. Kompotiatis, A. Kontogeorgakos, G. Kordas, J. Appl. Phys. 78 (1995) 3983–3991.
[27] P.-H. Martha, J. Magn. Magn. Mater 215 (2000) 171–183.
[28] T. Nakamura, J. Appl. Phys. 88 (2000) 348–353.